High-quality nonpolar 4H-AlN grown on 4H-SiC (11(2)over-bar20) substrate by molecular-beam epitaxy

AUTHOR(S):

Horita, M; Suda, J; Kimoto, T

CITATION:

Horita, M ...[et al]. High-quality nonpolar 4H-AlN grown on 4H-SiC (11(2)over-bar20) substrate by molecular-beam epitaxy. APPLIED PHYSICS LETTERS 2006, 89(11): 112117.

ISSUE DATE:

2006-09-11

URL:

http://hdl.handle.net/2433/39687

APPLIED PHYSICS LETTERS **89**, 112117 (2006)

High-quality nonpolar 4*H*-AlN grown on 4*H*-SiC (11$\bar{2}$0) substrate by molecular-beam epitaxy

Masahiro Horita,[a] Jun Suda, and Tsunenobu Kimoto
Department of Electronic Science and Engineering, Kyoto University, Kyotodaigaku-katsura, Nishikyo, Kyoto 615-8510, Japan

(Received 29 March 2006; accepted 21 July 2006; published online 13 September 2006)

Growth of very high-quality nonpolar (11$\bar{2}$0) *a*-plane face 4*H*-AlN on 4*H*-SiC (11$\bar{2}$0) substrate was investigated. Nonpolar 4*H*-AlN (11$\bar{2}$0) was isopolytypically grown on 4*H*-SiC (11$\bar{2}$0) substrate by molecular-beam epitaxy. A reduction of defects such as stacking faults and threading dislocations was achieved by keeping the growing surface flat. To this end, the SiC substrate was HCl gas etched and the V/III ratio was optimized for AlN growth. A full width at half maximum of symmetrical x-ray diffraction ω scan of the 4*H*-AlN layer was 40 arc sec. Transmission electron microscopy revealed the stacking fault density to be 2×10^5 cm^{-1}, and the partial and perfect threading dislocation densities to be 7×10^7 and 1×10^7 cm^{-2}, respectively. © *2006 American Institute of Physics*. [DOI: 10.1063/1.2352713]

Group-III nitride semiconductors such as gallium nitride (GaN) and aluminum nitride (AlN) with nonpolar growth direction, [11$\bar{2}$0] or [1$\bar{1}$00], have attracted much attention owing to their potential applications in high-efficiency light-emitting devices.[1] Various substrates for growth of nonpolar III-N have been investigated. Naturally, a III-N (11$\bar{2}$0) or (1$\bar{1}$00) substrate would be the best option.[2] However, obtaining large-size nonpolar wafers is rather difficult because of the plateletlike growth habit in bulk growth of III-N. Currently, sapphire (1$\bar{1}$02) *r*-plane, on which GaN (11$\bar{2}$0) is grown,[3,4] is widely used owing to its availability (3 in. diameter is commercially available) as well as its thermal stability in the nitride growth environment. Various groups have reported the growth of nonpolar GaN on sapphire (1$\bar{1}$02) by molecular-beam epitaxy (MBE),[5] metal-organic chemical vapor deposition (MOCVD),[6] and hydride vapor phase epitaxy.[7] However, due to the large structural mismatch [wurtzite (11$\bar{2}$0) on corundum (1$\bar{1}$02)] between nonpolar III-N and sapphire (1$\bar{1}$02), the quality of GaN grown on sapphire (1$\bar{1}$02) is inferior to that grown on sapphire (0001). For example, a stacking fault (SF) density of 4×10^5 cm^{-1} and a threading dislocation (TD) density of 3×10^{10} cm^{-2} were reported for MOCVD-grown GaN on sapphire (1$\bar{1}$02).[8] To improve the crystallinity, the epitaxial lateral-overgrowth technique was developed for nonpolar GaN. Haskell *et al.* reported a SF density of 3×10^3 cm^{-1} and a TD density of 5×10^6 cm^{-2} for the wing region.[9]

We focused on SiC (11$\bar{2}$0) and (1$\bar{1}$00) substrates for nonpolar AlN growth because of the following reasons. (1) Layer-by-layer growth of AlN in the initial stage is possible on SiC (0001), indicating good wetting of AlN on SiC.[10] (2) The lattice mismatch between AlN and SiC is much smaller than that between AlN and sapphire (1$\bar{1}$02). (3) Crystalline structure of SiC, 4*H* or 6*H*, resembles wurtzite more than it resembles sapphire (1$\bar{1}$02). To the author's knowledge, the first growth of nonpolar AlN on nonpolar SiC was performed by MBE by Stemmer *et al.*[11] They confirmed the epitaxial growth of 2*H*-AlN (1$\bar{1}$00) on 6*H*-SiC (1$\bar{1}$00). However, they did not report the crystal quality of AlN. We attempted to grow AlN on 6*H*-SiC (11$\bar{2}$0) and confirmed growth of 2*H*-AlN (11$\bar{2}$0).[12] We investigated the quality of the AlN layer. Full width at half maximum (FWHM) of the x-ray diffraction (XRD) ω scan was 240–3000 arc sec, which is comparable to that of GaN/sapphire (1$\bar{1}$02). We also attempted to grow AlN on 4*H*-SiC (11$\bar{2}$0). The AlN layer grown in this case exhibited far superior crystalline quality; its FWHM was 90 arc sec. Furthermore, reflection high-energy electron diffraction (RHEED) revealed that the AlN layer did not have the 2*H* structure, but rather the 4*H* structure, i.e., the same structure as the SiC substrate. The crystalline structure of the substrate was replicated in the grown layer. We speculate that the formation of the isopolytypic interface (no mismatch in crystalline structure between the AlN layer grown and the SiC substrate) may have resulted in such a high-quality AlN. Although XRD showed a very small FWHM value, high-resolution transmission electron microscopy (HRTEM) revealed that the 4*H*-AlN layer grown contained high-density SFs (5×10^6 cm^{-1}) and TDs (4×10^{10} cm^{-2}). Further reduction of SFs and TDs is necessary to use the 4*H*-AlN for device applications.

In the present study, we report growth of superior crystal quality 4*H*-AlN on 4*H*-SiC (11$\bar{2}$0). We have identified two critical factors that significantly improve the quality of 4*H*-AlN layers. The one is to prepare an atomically flat and damage-free 4*H*-SiC substrate surface, and the other is careful optimization of the V/III ratio. Since AlN tends to have the 2*H* structure, lateral growth along the [0001] direction may result in 2*H* inclusion, i.e., stacking faults. A very flat initial surface and optimized V/III ratio (slightly Al-rich conditions) ensure a very smooth grown surface, which prevents lateral growth and thereby leads to high phase purity.

The substrates used in this study were commercially available 4*H*-SiC (11$\bar{2}$0) wafers. Since the polishing process

[a]Electronic mail: horita@semicon.kuee.kyoto-u-ac.jp

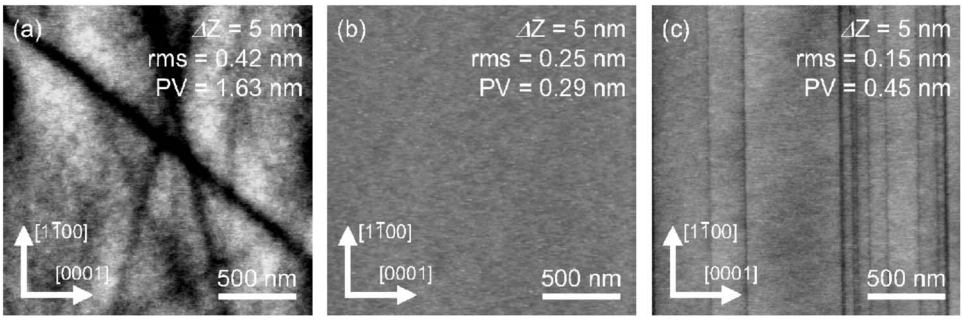

FIG. 1. 2×2 μm^2 atomic force microscopy scans for (a) as-received and (b) HCl-gas-treated 4*H*-SiC (11$\bar{2}$0) substrates and (c) a 230-nm-thick AlN epitaxial layer.

for 4*H*-SiC (11$\bar{2}$0) has not yet been established, many polishing scratches are observed on the wafer surface as shown in Fig. 1(a). The substrates were etched by a HCl–H_2 gas mixture at high temperature to remove the scratches. The etching conditions established for 6*H*-SiC (0001) substrates were used: temperature of 1300 °C, H_2 including 0.3% HCl, flow rate of 1 SLM (standard liters per minute), and etching time of 10 min.[13] After gas etching, a very smooth SiC surface [see Fig. 1(b)] was obtained, the rms roughness of which was below 0.3 nm. After this treatment, the substrates were dipped into a HF solution, rinsed by de-ionized water, and loaded into the MBE chamber. The MBE system was equipped with effusion cells for Ga and Al evaporations and a Veeco Unibulb rf plasma cell for producing active nitrogen (N^*). Prior to AlN growth, Ga deposition and desorption processes were performed to cleanse the SiC surface *in situ* of residual oxygen.[10] AlN growth was carried out at 950 °C under slightly Al-rich conditions: Al beam equivalent pressure of 9×10^{-7} Torr, N_2 flow rate of 1.0 SCCM (standard cubic centimeter per minute), and rf-plasma power of 400 W. The polytype of the AlN layer grown was confirmed to have the 4*H* structure by *in situ* RHEED observation. The typical growth rate was 400–500 nm/h. The crystalline quality was characterized by symmetrical and asymmetrical XRDs as well as HRTEM. HRTEM was performed by a JEOL JSM-2100F with the field-emission electron beam accelerated at 200 keV.

Figure 1(c) shows the surface morphology of a 230-nm-thick 4*H*-AlN (11$\bar{2}$0). A considerably smooth AlN layer with a rms roughness of 0.15 nm (2×2 μm^2) was obtained. Several line depressions were observed, whose density was $\sim1\times10^5$ cm^{-1}. The surface morphology was very different from that of 4*H*-AlN (1$\bar{1}$00) on 4*H*-SiC (1$\bar{1}$00). Elongated features were observed on 4*H*-AlN (1$\bar{1}$00) with a rms roughness of 0.9 nm. Surface migration on (11$\bar{2}$0) may be different from that on (1$\bar{1}$00).[14]

In XRD measurements, symmetrical (11$\bar{2}$0) reflection and asymmetrical (03$\bar{3}$0) and (11$\bar{2}$4) reflections were measured for a 470-nm-thick AlN layer. The results are summarized in Table I. For all reflections, the ω scan FWHM is less than 100 arc sec, indicating excellent crystalline quality. For the (11$\bar{2}$0) diffraction, the minimum value observed is 40 arc sec. In our previous study, in which neither HCl gas etching nor optimization of the V/III ratio nor Ga cleaning was performed, 4*H*-AlN with high-density stacking faults exhibited a FWHM of 90 arc sec.[12] The smaller FWHM values in the present study are indicative of lower SF and TD densities.

TABLE I. Full width at half maximum (arc sec) of x-ray $2\theta/\omega$ and ω scans for 470-nm-thick AlN on 4*H*-SiC (11$\bar{2}$0).

	$2\theta/\omega$ scan	ω scan
(11$\bar{2}$0)	143.2	39.8
(03$\bar{3}$0)	241.2	45.5
(11$\bar{2}$4)	161.4	76.1

Shown in Fig. 2(a) is a cross-sectional HRTEM image of the AlN layer. To observe the stacking structure by cross-sectional HRTEM, the [$\bar{1}$2$\bar{1}$0] zone axis, which is tilted by 60° from the growth direction ([11$\bar{2}$0]), was employed. The periodic structure of 4*H* polytype (*ABCBA*$\cdots$) with a lattice constant *c* of 1.0 nm was clearly observed. It should be noted that there are no SFs within the observed area. SFs can be observed in a lower-magnification image (not shown here), on the basis of which the SF density was estimated to be 2×10^5 cm^{-1}. For reference, the image of 4*H*-AlN previously reported is shown in Fig. 2(b),[12] where two bundles of SFs are observed. The SF density is approximately 5×10^6 cm^{-1} and could be dramatically reduced in the present study. Since the SF density almost agrees with the density of line depressions observed in the AFM image, the line depression may be a growth defect originating from a SF.

To evaluate the TD density, plan-view TEM observation was carried out. Figure 3(a) and 3(b) show the bright field images of a 4*H*-AlN epilayer with $\boldsymbol{g}=1\bar{1}00$ and $\boldsymbol{g}=0004$,

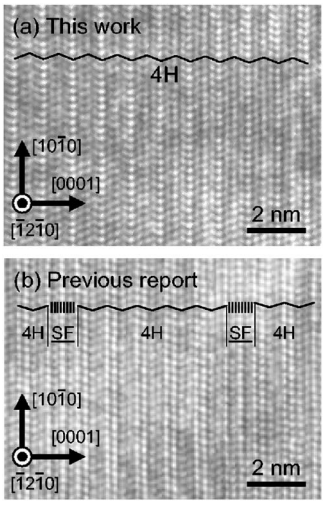

FIG. 2. Cross-sectional high-resolution transmission electron microscopy images of AlN grown on 4*H*-SiC (11$\bar{2}$0) in (a) the present study and (b) our previous study (Ref. 12).

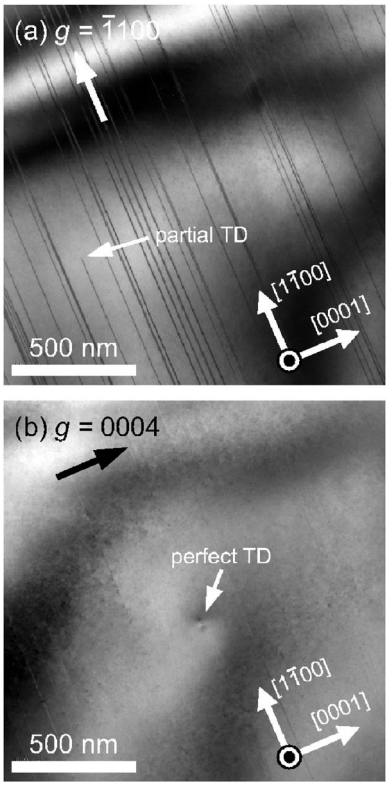

FIG. 3. Bright field plan-view TEM images of AlN grown on 4*H*-SiC $(11\bar{2}0)$ under the (a) $\boldsymbol{g}=1\bar{1}00$ and (b) $\boldsymbol{g}=0004$ diffraction conditions.

respectively. Dark lines running along $[1\bar{1}00]$ correspond to stacking faults in the TEM image under the $\boldsymbol{g}=1\bar{1}00$ diffraction condition [Fig. 3(a)]. Since a partial TD exists at the end of the SF,[15] the density of partial TDs having Burgers vectors $\boldsymbol{b}=\frac{1}{3}\langle 1\bar{1}00\rangle$ is estimated at about 7×10^7 cm^{-2} by examining a wider area of 22 μm^2. A perfect TD was observed in the TEM image under the $\boldsymbol{g}=0004$ diffraction condition [Fig. 3(b)]. Two perfect TDs were found in an area of 22 μm^2, indicating that the density of TDs having [0001] component is about 1×10^7 cm^{-2}. These TD densities are extremely small for heteroepitaxial AlN on any substrates. XRD shows a very sharp diffraction peak as mentioned above, supporting this result.

Table II shows the in-plane and out-of-plane (growth-direction) lattice constants of AlN epilayer and SiC substrate measured by XRD. The in-plane lattice constants of AlN are equal to those of SiC (to within an error of 0.1%), indicating that the AlN layer grows on the SiC substrate almost pseudomorphically. Pseudomorphic growth may contribute such a low dislocation density.

In conclusion, we have performed the growth of high crystal quality AlN on 4*H*-SiC $(11\bar{2}0)$ substrates by using an atomically flat SiC surface and optimized V/III ratio. The AlN grown was found to be high-phase purity 4*H*-AlN. Symmetric and asymmetric XRD ω scans showed very sharp peaks with FWHM of less than 100 arc sec. Density of the basal plane SFs was estimated to be 2×10^5 cm^{-1}, and densities of partial and perfect TDs to be 7×10^7 and 1×10^7 cm^{-2}, respectively. The SF and TD densities of 4*H*-AlN were reduced by two orders of magnitude, compared to that of the 4*H*-AlN previously reported. High-quality 4*H*-AlN grown on 4*H*-SiC $(11\bar{2}0)$ is a very promising template for future deep-UV high-Al-composition AlGaN optical devices.

TABLE II. Lattice constants of AlN epilayer and SiC substrate measured by XRD.

	AlN (Å)	SiC (Å)	Difference (%)
$d_{(0001)}$	10.032	10.042	−0.10
$(2/\sqrt{3})d_{(1\bar{1}00)}$	3.079	3.082	−0.10
$2d_{(11\bar{2}0)}$	3.105	3.081	+0.78

This work was supported by the 21st Century Center of Excellence (COE) Program (Grant No. 14213201).

[1] P. Waltereit, O. Brandt, A. Trampert, H. T. Grahn, J. Menniger, M. Ramsteiner, M. Reiche, and K. H. Ploog, Nature (London) **406**, 865 (2000).
[2] H. Teisseyre, C. Skierbiszewski, B. Lucznik, G. Kamler, A. Feduniewicz, M. Siekacz, T. Suski, P. Perlin, I. Grzegory, and S. Porowski, Appl. Phys. Lett. **86**, 162112 (2005).
[3] T. Sasaki and S. Zembutsu, J. Appl. Phys. **61**, 2533 (1987).
[4] C. R. Eddy, Jr., T. D. Moustakas, and J. Scanlon, J. Appl. Phys. **73**, 448 (1993).
[5] H. M. Ng, Appl. Phys. Lett. **80**, 4369 (2002).
[6] M. D. Craven, F. Wu, A. Chakraborty, B. Imer, U. K. Mishra, S. P. DenBaars, and J. S. Speck, Appl. Phys. Lett. **84**, 1281 (2004).
[7] B. A. Haskell, F. Wu, S. Matsuda, M. D. Craven, P. T. Fini, S. P. DenBaars, J. S. Speckand, and S. Nakamura, Appl. Phys. Lett. **83**, 1554 (2003).
[8] H. Wang, C. Chen, Z. Gong, J. Zhang, M. Gaevski, M. Su, J. Yang, and M. A. Khan, Appl. Phys. Lett. **84**, 499 (2004).
[9] B. A. Haskell, F. Wu, M. D. Craven, S. Matsuda, P. T. Fini, T. Fujii, K. Fujito, S. P. DenBaars, J. S. Speck, and S. Nakamura, Appl. Phys. Lett. **83**, 644 (2003).
[10] N. Onojima, J. Suda, and H. Matsunami, Jpn. J. Appl. Phys., Part 2 **42**, L445 (2003).
[11] S. Stemmer, P. Pirouz, Y. Ikuhara, and R. F. Davis, Phys. Rev. Lett. **77**, 1797 (1996).
[12] N. Onojima, J. Suda, T. Kimoto, and H. Matsunami, Appl. Phys. Lett. **83**, 5208 (2003).
[13] S. Nakamura, T. Kimoto, and H. Matsunami, Appl. Phys. Lett. **76**, 3412 (2000).
[14] R. Armitage, J. Suda, and T. Kimoto, Appl. Phys. Lett. **88**, 011908 (2006).
[15] R. Liu, A. Bell, F. A. Poncea, C. Q. Chen, J. W. Yang, and M. A. Khan, Appl. Phys. Lett. **86**, 021908 (2005).